Journal of Plant Growth Regulation (2023) 42:2519–2529
https://doi.org/10.1007/s00344-022-10723-0

Phytohormones in Sweet Cherry Buds During Winter Rest and Bud Development

Klaus-Peter Götz[1] · Frank-M. Chmielewski[1] · Danuše Tarkowská[2] · Aleš Pěnčík[2] · Ondřej Novák[2]

Received: 18 January 2022 / Accepted: 1 July 2022 / Published online: 21 July 2022

Abstract

This (two-season) study was undertaken to assess the involvement of gibberellins (GAs), cytokinins (CKs), and auxins (AX) in dormancy of the sweet cherry buds 'Summit'. Our hypothesis consisted in the assumption that representatives of these hormone groups are able to mark the transition between different dormancy phases. Changes in the transition between endo- and ecodormancy and the stages of ontogenetic development were not recognizable by bioactive GA_1, GA_5, GA_7. The transient increase of GA_3 during ecodormancy might be interpreted as an indication of the preservation of ecodormancy. The content of the biological active bases *t*Z, *c*Z, and DHZ was equal between endo- and ecodormancy. However, the content increased significantly in the first phase of ontogenetic development. The summation of the representatives of the various CKs (total iP-type, total *t*Z-type, total CK bases, total CK ribosides, total CK nucleotides, total *O*-glucosides, total *N*-glucosides, and total CKs) showed no differences regarding their levels during endo- and ecodormancy. These values increased markedly in the subsequent phase. AX increased after ecodormancy. By contrast, from side green until open cluster no differences occurred. As shown for AX, the content of oxIAA increased after ecodormancy. The content of IAAsp was low during endodormancy and increased transiently during ecodormancy and early ontogenetic development. This study revealed that no changes in the content of different bioactive GAs (exception GA_3), CKs, and AX occurred during winter rest, and more precisely, during endo- and ecodormancy. These metabolites, therefore, are not suitable to differentiate between these dormancy phases. The ontogenesis is accompanied by specific changes in the content of bioactive molecules, precursors, and conjugation products.

Keywords Flower buds · *Prunus avium* L. · Gibberellins · Cytokinins · Auxins

Introduction

Many endogenous signalling and regulatory molecules, like plant hormones, can be found in plants that regulate growth and development. The hormone family includes abscisic acid (ABA), auxin (AX), brassinosteroids (BRs), cytokinins (CKs), ethylene, gibberellins (GAs), salicylic acid (SA), strigolactones, and jasmonates (JAs). These molecules operate at very low concentrations and were synthesized from common metabolic precursors, and each uses uniquely specialized pathways. Their generation is strictly controlled, both spatially and temporally. All hormones influence multiple aspects of plant function, and they influence the synthesis and actions of each other. The interactions amongst hormones, environmental signals, and developmental programs are very complex, and as a result, the description and modelling of the whole system are quite challenging (Smith et al. 2017). Some hormone receptors are membrane-anchored (*e.g.* CKs) whilst others are soluble (*e.g.* AX, GAs). Hormone perception can lead to signal transduction through protein phosphorylation cascades (*e.g.* ABA, CKs). Other hormone-receptor complexes trigger interaction with F-box proteins and ubiquitination enzymes that target proteins such as transcriptional repressors for degradation by the 26S proteasome (*e.g.* AXs, GAs). Such signalling changes protein activities and gene transcription, with consequent changes to plant development and physiology (Smith et al. 2017).

Handling Editor: Nicola Busatto.

✉ Klaus-Peter Götz
klaus-peter.goetz@agrar.hu-berlin.de

[1] Agricultural Climatology, Faculty of Life Sciences, Humboldt-University of Berlin, Albrecht-Thaer-Weg 5, 14195 Berlin, Germany

[2] Laboratory of Growth Regulators, Institute of Experimental Botany, The Czech Academy of Sciences & Faculty of Science, Palacký University, Šlechtitelů 27, 78371 Olomouc, Czech Republic

The main physiological effects of biologically active GAs are well-known and include the induction of germination and floral transition, leaf expansion, and stimulation of stem elongation through enhanced cell division and elongation. Many GAs, have been reported in plants, but only GA_1, GA_3, GA_4, GA_5, and GA_7 function as bioactive hormones, whereas non-bioactive forms act either as precursors or degradation products of the bioactive ones (Hedden and Phillips 2000; Urbanová et al. 2013; Barboza-Barquero et al. 2015; Campos-Rivero et al. 2017 and references therein). Although it is essential to know the concentrations of the bioactive forms of GAs, knowledge of the concentrations of their precursors and metabolites provides physiological information concerning GA metabolism and its regulation by, for example, genetic or environmental factors (Urbanová et al. 2013). CKs are N^6-substituted purine-derived molecules that function as growth regulators and are involved in many developmental and physiological processes. CKs participate in regulating numerous aspects of plant development throughout the life cycle. These include seed germination, chloroplast differentiation, differentiation of vascular tissue, apical dominance (shoot branching), nutritional signalling, regulation of sink strength, the transition from the vegetative to the reproductive growth phase, and also flower and fruit development (Zalabák et al. 2013). The involvement of CKs during floral transition has not been defined completely, but it is known that they control cell division and differentiation in the floral meristem. During post-embryonic development, CKs are required to maintain meristem activity and leaf development in the plant shoot (Schmülling 2004; Campos-Rivero et al. 2017 and references therein). Whilst the biosynthetic pathway of the isoprenoid CKs and their subsequent metabolic conversions have been described in detail, respective genes cloned and physiological consequences of their loss-of-function or overexpression are well documented, the information about the biosynthesis of aromatic CKs remains elusive. Auxins are necessary for normal plant growth and development, as they regulate a variety of developmental processes such as cell elongation and division, organ patterning, root and shoot development, and tropic responses to light and gravity. In higher plants, the main natural auxin is indole-3-acetic acid (IAA), which is synthesized in young leaves, cotyledons, expanding leaves, and root tissues. However, indole-3-butyric acid (IBA) and 4-chloroindole-3-acetic acid (4-Cl-IAA) are also natural auxins (Campos-Rivero et al. 2017 and references therein). AX biosynthesis in plants is complex, and several pathways contribute to de novo IAA production. Notable also is that auxin biosynthesis is regulated by both environmental and developmental signals. Moreover, DELLA proteins inhibit flowering, and these proteins can be positively or negatively regulated by GAs and IAA (Zhao 2010). The switch from vegetative to reproductive growth, also known as the floral transition, is controlled by both endogenous and exogenous cues, such as temperature, photoperiod, and multiple hormones. Molecular and genetic analyses have revealed that the multiple floral inductive cues are integrated via a set of floral-promoting MADS-box genes, including APETALA1 (AP1), SUPPRESSOR OF OVEREXPRESSION OF CO1 (SOC1), FRUITFUL (FUL), and the plant-specific transcription factor LEAFY (LFY) (Yu et al. 2012 and references therein).

The dormancy of fruit trees is associated with invisible growth and development. It comprises endodormancy, triggered by internal factors, and ecodormancy, controlled by external factors. The release of endodormancy requires cold accumulation, whereas ecodormancy advances with warm temperatures towards bud break (Van der Schoot et al. 2014; Chmielewski and Götz 2017; Beauvieux et al. 2018). Reviews from Campoy et al. (2011) and Koutinas et al. (2010) gave an excellent overview of dormancy and flower bud development of temperate fruit trees. Beauvieux et al. (2018) reviewed both early and recent findings on the dormancy processes in buds of temperate fruit trees species. These include hormonal signalling, carbohydrate metabolism, the role of the plasma membrane, mitochondrial respiration, and oxidative stress, with an effort to link them together and emphasize the central role of ROS accumulation in the control of endo- and ecodormancy. Usually, there is no precise information regarding the date of endodormancy release (t_1) or the beginning of ontogenetic development (t_1*). After completing leaf fall, sweet cherry trees (cv. 'Summit') stopped acquiring measurable effects of bud growth. From this date, physiological parameters reached a constant level (Leaf fall-t_1: Water content = 53.5%, Fresh weight = 61.9 mg/bud, Dry weight = 28.8 mg/bud, Nitrogen content = 1.6%, Carbon content = 49.6%, mean of 6 seasons), which did not change significantly in individual seasons until t_1* (Chmielewski and Götz 2017). Results from several fruit tree studies emphasize the implication of plant hormones in the control of dormancy, although only a few studies quantified them directly in the compartment 'bud'. Therefore, this two-season study was undertaken to assess the involvement of GAs, CKs, and AX under natural conditions during different phenological phases of sweet cherry buds from 'leaf fall' until the 'open cluster' development stage. Our hypothesis consisted in the assumption that representatives of these hormone groups are able to mark the transition between the different dormancy phases, which then can used as physiological parameter to improve phenological models for the not observable dates of endodormancy release (t_1) and/or the beginning of ontogenetic development (t_1*).

Materials and Methods

The study was conducted during the 2012/13 and 2013/14 growing seasons in the Experimental Sweet Cherry Orchard at Humboldt-University in Berlin-Dahlem (52° 28' Northern latitude and 13° 18' Eastern longitude). The long-term (1981–2010) average annual air temperature and precipitation are 9.9 °C and 562 mm, respectively. We examined the cultivar 'Summit', originating at Summerland (British Columbia) in Canada, which is a mid-to-late maturing sweet cherry cultivar with dense crowns. It is a product of the crossover Van x Sam (1957, German Gene Bank Fruit). Summit was grafted on rootstock GiSelA 5 (Giessener Selektion Ahrensburg), a weakly- to medium-strongly growing stock.

The release of endodormancy (t_1) and the beginning of ontogenetic development (t_1*) are not visible, so we estimated t_1 and t_1* as follows: observing twigs under controlled conditions, which indicate the release of endodormancy (t_1, Chmielewski and Götz 2017), and measuring the water content of buds from the orchard. The first sign of the transition from the dormant stage to the beginning of ontogenetic development (t_1*) was found in changes in the bud's water content (Götz et al. 2014; Chmielewski and Götz 2017). The increase of the water content in the buds through the two seasons, from ~55% to ~80%, was related to a rise in air temperature from t_1* until the open cluster.

Bud Sampling

Samples of three clusters from each tree ($n = 3$) were taken at random locations over the whole tree, weekly, and from October to March. After visible bud development (March) sampling was done at the development stages 'swollen bud' (SB), 'side green' (SG), 'green tip' (GT), 'tight cluster' (TC), and at 'open cluster' (OC). After cutting, the clusters were immediately placed on ice, and 4 to 7 buds were selected, except for the smaller leaf bud in the middle, frozen in liquid nitrogen, and stored at −80 °C until freeze-drying. All buds were ground in a ball mill (Retsch M1, Haan, Germany) before analysis.

Sampling of Twigs

Young, multi-branched twigs (length about 25 cm, diameter 5 mm) with 2–3 clusters from other trees of 'Summit' were cut weekly during each year (November-December) to visually observe the beginning of blossom of the cluster under controlled conditions. After cutting, twigs were placed in 500 ml plastic flasks with demineralized water and kept in a controlled climate chamber (RUMED, Rubarth Apparate GmbH, Germany) (air temperature ~20 °C/15 °C day/night, 12 h light, relative humidity 70%). We assumed that the chilling requirement was sufficient if 3–4 flowers per twig did completely open (BBCH 60), on both the first and the following samplings.

Quantitative Analysis of Gibberellins, Cytokinins, and Auxins

The sample preparation and analysis of GAs was performed according to the method described in Urbanová et al. (2013) with some modifications. Briefly, tissue samples of about 30 mg dry weight (DW) were ground to a fine consistency using 2.7-mm zirconium oxide beads (Retsch GmbH & Co. KG, Haan, Germany) and a MM 400 vibration mill at a frequency of 30 Hz for 3 min (Retsch GmbH & Co. KG, Haan, Germany) with 1 ml of ice-cold 80% acetonitrile containing 5% formic acid as extraction solution. The samples were then extracted overnight at 4 °C using a benchtop laboratory rotator Stuart SB3 (Bibby Scientific Ltd., Staffordshire, UK) after adding internal gibberellins standards ($[^2H_2]GA_1$, $[^2H_2]GA_3$, $[^2H_2]GA_4$, $[^2H_2]GA_6$, $[^2H_2]GA_7$, $[^2H_2]GA_8$, $[^2H_2]GA_9$, $[^2H_2]GA_{15}$, $[^2H_2]GA_{19}$, $[^2H_2]GA_{20}$,$[^2H_2]GA_{24}$, $[^2H_2]GA_{29}$, $[^2H_2]GA_{34}$, $[^2H_2]GA_{44}$, $[^2H_2]GA_{51}$, and $[^2H_2]GA_{53}$ purchased from OlChemIm, Czech Republic. The homogenates were centrifuged (at 19.000 rotation per minute (rpm), for 10 min, at 4 °C; Beckman Avanti™ 30), the corresponding supernatants further purified using reversed-phase and mixed-mode SPE cartridges (Waters, Milford, MA, USA) and analysed by ultra-high-performance liquid chromatography-tandem mass spectrometry (UHPLC-MS/MS; Micromass, Manchester, UK). GAs were detected using multiple reaction monitoring mode of the transition of the ion $[M–H]^-$ to the appropriate product ion. Masslynx 4.2 software (Waters, Milford, MA, USA) was used to analyse the data and the standard isotope dilution method (Rittenberg and Foster 1940) was used to quantify the GAs levels.

Endogenous levels of CKs, free IAA (indole-3-acetic acid), its catabolite (oxIAA) and indole-3-acetyl aspartate (IAAsp) were determined by LC–MS/MS methods (Novák et al. 2008, 2012). Approximately 5 mg (dry weight) of plant tissue were homogenized and extracted in 1 ml of modified Bieleski buffer (60% MeOH, 10% HCOOH and 30% H_2O). A mix of stable isotope-labelled internal standards (0.25 pmol of CK bases, ribosides, N-glucosides, 0.5 pmol of CK *O*-glucosides and nucleotides, 5 pmol of $[^{13}C_6]$ IAA, and $[^{13}C_6]$ oxIAA and $[^{13}C_6]$ IAAsp was added to each sample to validate phytohormone determination (Novák et al. 2008). The extracts were purified using two solid-phase extraction columns, the octadecyl silica-based column (C18, 500 mg of sorbent, Applied Separations), and that of the Oasis MCX column (30 mg/1 ml, Waters) (Dobrev and Kamínek 2002). Analytes were eluted by three-step elution

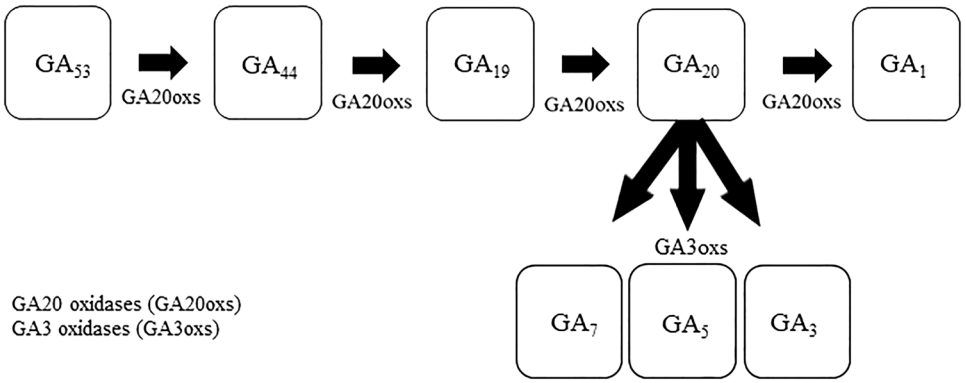

Fig. 1 Simplified GA biosynthesis pathway of 13-hydroxylated GAs

using a 60% (v/v) MeOH, 0.35 M NH_4OH aqueous solution and 0.35 M NH_4OH in 60% (v/v) MeOH solution. CK, free IAA, oxIAA, and IAAsp levels were determined using ultra-high-performance liquid chromatography-electrospray tandem mass spectrometry (an Acquity UPLC I-Class System coupled to a Xevo TQ-S MS, all from Waters) using stable isotope-labelled internal standards as a reference (Rittenberg and Foster 1940).

Statistical Analysis

The data were separately analysed for the three phenological phases, 'leaf fall (LF)-end of endodormancy (t_1)', 'ecodormancy (t_1)-beginning of ontogenetic development (t_1*)', and ontogenetic development (t_1*)-swollen bud', and the visible phenological stages 'side green', 'green tip', 'tight' and 'open cluster' (mean, standard error (SE), ANOVA, Scheffé's procedure, a very conservative adjustment, which allows a statistical analysis of an unequal number of repetitions, $p \leq 0.05$) using statistical software IBM SPSS Statistic 25.0). Furthermore, data for the two years were pooled because of measurement similarities that were obtained for the two seasons.

Results and Discussion

The mean air temperature (2012/13, 2013/14) during the phenophases endodormancy 'leaf fall—end of endodormancy (t_1)', ecodormancy 't_1—beginning of ontogenetic development (t_1*)', and during ontogenetic development t_1*—swollen bud, swollen bud—side green, side green—green tip, tight cluster—open cluster, was 6.4, 1.6, 3.4, 8.0, 13.0, 10.2, and 11.8 °C, respectively.

Gibberellins (GAs)

Eighteen GAs were verifiably detected in the buds (data not shown) compared to 23 GAs found in *Arabidopsis thaliana*, 14 GAs in oilseed rape (*Brassica napus*), and 12 GAs in rice (*Oryza sativa*) (Urbanova et al. 2013). A simplified overview of the pathway of their biosynthesis, including bioactive compounds GA_1, GA_3, GA_5, and GA_7 (Hedden and Phillips 2000; Yamaguchi 2008; Weiher et al. 2014; Pietlot et al. 2015), formed from the precursor GA_{53} is shown in Fig. 1, along with their concentrations in the sweet cherry buds (Fig. 2). The GA_{53} content (Fig. 2A) was in the range between 1.51 pg/mg (LF-t_1) and 2.96 pg/mg (SG), and statistically not different between phenological phases and stages. GA_{53} was oxidized in three steps step by step into GA_{44} (Fig. 2B), GA_{19} (Fig. 2C), and GA_{20} (Fig. 2D) by GA-20 oxidases (GA20oxs), belonging to the class of the 2-oxoglutarate dependent dioxygenases (2ODDs).

Between LF and SB, the GA_{44} content was similar, having 4.80 pg/mg on average (Fig. 2B), and reaching a maximum of 11.45 pg/mg at SG, which was clearly higher than at GT and TC, 2.82, 2.36 pg/mg, respectively. In the same phase (LF-SB) the mean GA_{19} content (Fig. 2C) was very low (0.61 pg/mg), and decreased further to its minimum of 0.38 pg/mg at SG, and then was followed by a strong (3.6, 4.6, 5.4-fold) increase of oxidation by growth and development of the buds at GT, TC, and OC, respectively.

The GA_{20} content (Fig. 2D) was found in the range between 0.66 (LF-t_1) and 0.28 pg/mg (OC), and was statistically not different within the phenological phases and stages. The formation of bioactive compounds is catalyzed by a GA 3-oxidases (GA3oxs) (Fig. 1, Hedden and Thomas 2012). Independent of the phenological phase or the developmental stage, the content of the bioactive GA_1, GA_5, and GA_7 was not different from leaf fall until the open cluster (Fig. 2E, G, H). The mean GA_1 content of 1.2 pg/mg (Fig. 1E) between LF (beginning of endodormancy) and SB (significant increase of the water content) was tendentially 3.3-fold higher than the content at the growth stages GT, TC, OC, with 0.36 pg/mg on average. This trend agrees with Beauvieux et al. (2018), who reported that the highest levels of GA_1 and GA_3 were found in dormant buds during endodormancy release, whereas the content diminished afterwards.

The mean GA_3 and GA_5 content (Fig. 2F, G) of 0.5 pg/mg and 0.6 pg/mg between LF and OC was comparable, whereas the mean GA_7 content, with 0.08 pg/mg, was the lowest of the bioactive GAs (Fig. 2H). Interestingly, for GA_3 a significant increase to 0.74 pg/mg was observed during ecodormancy (t_1-t_1*), compared to mean values of 0.50 pg/mg during endodormancy (LF-t_1) and the beginning of ontogenetic development (t_1*-SB). In summary, changes in the transition between endo- and ecodormancy and the stages of ontogenetic development were not recognizable by bioactive GA_1, GA_5, and GA_7. However, the transient increase of GA_3 during ecodormancy might be interpreted as an indication of the preservation of ecodormancy in the sweet cherry buds.

Cytokinins (CKs)

CK biosynthesis is initiated by the activity of isopentenyltransferases (IPTs). Monophosphorylated CK nucleotides can be directly converted into free bases by the activity of cytokinin nucleoside 5′-monophosphate phosphoribohydrolases (LOG). Active CKs (isopentenyladenine (iP), *trans*-zeatin (*t*Z), *cis*-zeatin (*c*Z), and dihydrozeatin (DHZ)) and their respective ribosides (~R) can be inactivated by CK oxidases/dehydrogenases (CKX), or by the formation of sugar conjugates (*O*-glucosides (~OG), riboside *O*-glucosides (~ROG), N7-glucosides (7~G), and N9-glucosides (~9G)) through the activity of glycosyltransferases, like zeatin *O*-glucosyltransferase or N-glucosyltransferases (ZOG, UGT) (Schäfer et al. 2015a, b; Zalabák et al. 2013 and references therein). In *Arabidopsis thaliana*, the isopentenyl group is derived from the mevalonate (MVA) pathway in the cytosol. However, the predicted localization of enzymes in other plants suggests the use of isoprene moieties derived from the methylerythritol phosphate (MEP) pathway. Therefore, the MEP pathway also contributes to iP and *t*Z biosynthesis (Schäfer et al. 2015a, b).

In the sweet cherry buds 23 CK-related metabolites could be detected (data not shown). Free CK bases (Table 1) are cytokinin species that most strongly bind to cytokinin receptors. The binding is associated with physiological responses; thus, these forms are considered biologically active (Rijavec and Deamastia 2010). The iP content increases stepwise (from 2.2 to 4.8 to 6.3) from endodormancy, ecodormancy, and to the phase t_1*-SB, respectively, whereas the later content was higher during endodormancy (LF-t_1). Originally, cytokinin biosynthesis was reported to take place exclusively in roots, and it was shown that CKs could be transported in the xylem from the root to the shoot to stimulate shoot growth. However, more recent work provided evidence that CKs can be synthesized also in aerial plant parts. Measurements of xylem and phloem exudates confirmed this observation and showed that the phloem contains mainly iP-type CKs, whereas xylem sap contains mainly *t*Z-type CKs (Kang et al. 2017 and references therein). The content of the biological active bases *t*Z, *c*Z, and DHZ were equal between endo- and ecodormancy: however, content increased significantly in the following phases t_1*-SB to 4.1, 3.7, 1.2 pmol/g DW, respectively. Therefore, it is not possible to differentiate between endo- and ecodormancy based on these free CK bases. Also, this shows clearly that the activity of the enzymes involved in *t*Z, *c*Z, and DHZ synthesis does not change until the phase t_1*-SB and/or transport via the vascular system takes place.

During bud development SG to OC (Table 1) the free base *t*Z was the dominant form with mean values of 24 pmol/g DW, followed by iP and *c*Z, 15 and 7 pmol/g DW, respectively, and was statistically not different between the stages of development. DHZ increase markedly from ~2 pmol/g DW (mean SG, GT) to ~8 pmol/g DW after GT (mean TC, OC). The content of their respective ribosides (Table 2) iPR, *t*ZR, *c*Z were equal between endo- and ecodormancy (~9, ~4, ~10 pmol/g DW); however, increased markedly in the following phase t_1*-SB to 25.0, 8.0, 24.1 pmol/g DW, respectively, which was fourfold, twofold, sevenfold higher, compared to the free bases during this phase (Table 1). The development of buds (SG-OC) was accompanied by a significant increase in ribosides. The highest mean levels were achieved for iPR, *t*ZR, *c*Z at GT and TC (~297, ~447, ~202 pmol/g DW), where *t*ZR is the dominant form here, too. The DHZR content of 117 pmol/g DW shows a temporary maximum at TC, compared to SG/GT and OC.

As already mentioned, the formation of sugar conjugates, N9-glucosides and *O*-glucosides, respectively, (Table 3) lead to the inactivation of CKs. The content of iP9G was below 1 pmol/g DW and similar between LF and SB and between SG and OC. The *t*ZOG content was also similar between LF and SB, and SG and OC, ~41 pmol/g DW and 71 pmol/g DW, respectively, representing, therefore, a stable pool in each of the phenological phases and during bud development stages. In comparison, the *c*ZOG content was steadily increasing from endo- to ecodormancy, and to the phase t_1*-SB, 28, 46, 65 pmol/g DW, respectively. From SG onwards the *c*ZOG content of 107.4 pmol/g DW was decreasing stepwise to 75.3, 46.0, 39.3 pmol/g DW at GT, TC, and OC, respectively, indicating a reducing pool size during bud development for this metabolite. The content of DHZOG differed clearly between endodormancy and the phase t1*-SB, 24.6, 28.6 pmol/g DW, respectively; and shows a similar mean content of 28 pmol/g DW between SG and OC.

The *c*ZROG content (Table 4) was on average 1.8 pmol/g DW and similar between endo- and ecodormancy, and showed an increase during t_1*-SB to 3.3 pmol/g DW, whereas the content of *t*ZROG and DHZROG, with mean values of 1.4, 1.6 pmol/g DW, respectively, was stable from

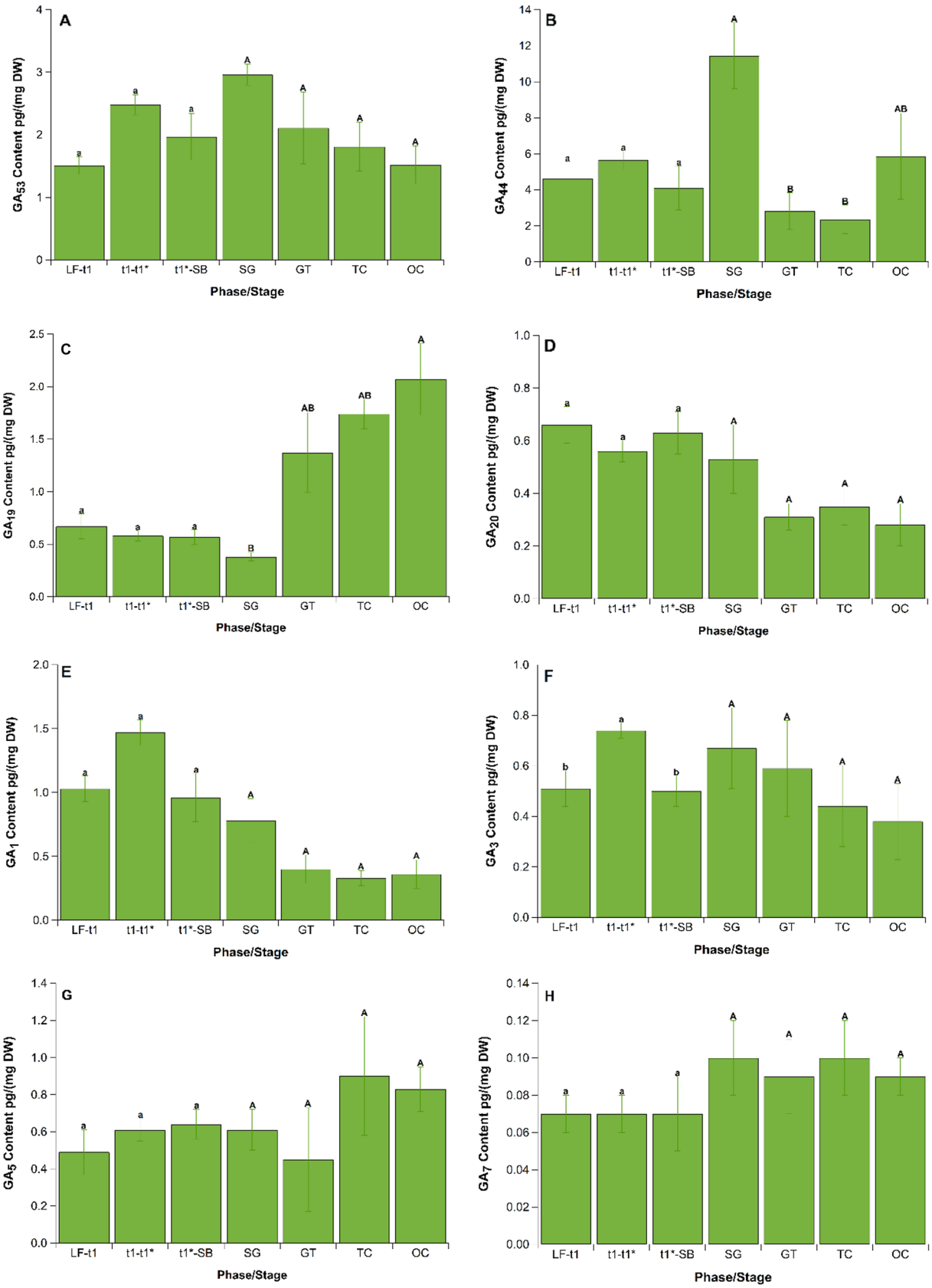
A
GA53 Content pg/(mg DW)
B
GA44 Content pg/(mg DW)
C
GA19 Content pg/(mg DW)
D
GA20 Content pg/(mg DW)
E
GA1 Content pg/(mg DW)
F
GA3 Content pg/(mg DW)
G
GA5 Content pg/(mg DW)
H
GA7 Content pg/(mg DW)
LF-t1
t1-t1*
t1*-SB
SG
GT
TC
OC
Phase/Stage

◂**Fig. 2** **A**–**H** Contents of GA_{53}, GA_{44}, GA_{19}, GA_{20}, GA_1, GA_3, GA_5, GA_7 in sweet cherry buds during different phases and at different phenological stages. (Mean ± SE 2012/13 and 2013/14, ANOVA, Scheffé's procedure; different small letters indicate significance ($p < 0.05$) between phenological phases and capitals between phenological stages

leaf fall until SB. *c*ZROG had a significantly higher content at TC and OC of 10.5 pmol/g DW on average, in comparison with SG and GT. Compared to TC and OC *t*ZROG shows a lower content at SG and GT, whereas DHZROG shows no clear differences between SG and OC.

The summation of the representatives of the various CKs (Table 5), total iP-type, total *t*Z-type, total CK bases, total CK ribosides, total CK nucleotides, total *O*-glucosides, total *N*-glucosides, and the total CKs showed no differences regarding their levels during endo- and ecodormancy. Only in the subsequent phase, from the beginning of ontogenetic development to SB, these values were found to increase significantly (2.6, 1.4, 1.9, 2.3, 2.0, 1.3, 1.2, 1.6-fold) to 44, 68, 15, 61, 50, 140, 2, and 268 pmol/g DW, respectively. As an exception, the total *c*Z-type showed clear differences amongst the three phases endodormancy, ecodormancy, and the beginning of ontogenetic development to SB with 57, 79, and 124 pmol/g DW, respectively. To activate the CK-specific phosphorelay, *c*Zs should be able to bind and activate the CHASE-domain containing histidine kinases (CHKs), which serve as CK receptors. Indeed, it could be shown that *c*Zs can bind to CHKs and activate downstream elements of the signalling cascade, although with different sensitivity, depending on the plant species and the specific receptor (Schäfer et al. 2015a, b and references therein). Results of different plant species reveal that *c*Z-type CKs tend to accumulate under the prevailing circumstances, associated with limited growth or dormancy, as is found in buds, tubers, and seeds. However, a stronger and increasing accumulation of the total CKs (with one exception, the total CK *N*-glucosides) was clearly associated with the flower bud development from SG to OC. However, the CK content remained similar for the total *c*Z-type, total CK bases, and total CK *O*-and *N*-glucosides (Table 5). During the GT and TC stages, the highest values (in comparison to SG and TC) were temporarily achieved for the total iP-type, total *t*Z-type, total CK ribosides, total CK nucleotides, and the total CKs, whereas for the total DHZ type the highest content was acquired at TC and OC (Table 5). Over the past decade, many genes have been identified that affect CK synthesis, transport, metabolism, and perception. In Arabidopsis, it appears that a gene family of more than 50 members controls all these processes (Zabalak et al. 2013 and references therein). These data, on the levels of specific CKs during phenological phases, leaf fall via the break of dormancy (endodormancy), the not-visible beginning of ontogenetic development until SB (ecodormancy), and the subsequent phenological stages SG, TC, and OC, should contribute to a better understanding of the CKs in sweet cherry buds.

Auxin

The regulation of IAA in plants, as for other phytohormones, is also a complex process. The principal auxin metabolic pathways in seed plants is comprehensively reported by Kramer and Ackelsberg (2015).

The mean IAA content in the buds between leaf fall and t_1* was 269 pmol/g DW (Table 6). IAA increased clearly after ecodormancy (246.0 pmol/g DW) during the following phase until SB (337.1 pmol/g DW), whereas during the developmental stages from side green until open cluster (range of 174.7 – 556.2 pmol/g DW) no differences occurred.

IAA oxidation and conjugation are two different pathways that inactivate IAA. Enzymes as DIOXYGENASE OF AUXIN OXIDATION (DAO) catalyzing the oxidative reaction, were characterized in *Arabidopsis thaliana* (Zhang and Peer 2017). This highly diverse protein family is involved in many growth and developmental processes, as e.g. hormone synthesis and breakdown and flavonoid biosynthesis, but also responses to the environment. Detailed information about auxin homeostasis, simplified auxin biosynthesis, conjugation, and non-decarboxylation oxidation pathways is presented by Zhang and Peer 2017. The mean oxIAA content in the buds (Table 6) from leaf fall until t_1*, was 240 pmol/g DW. As shown for IAA, the content of oxIAA increased clearly after ecodormancy during the following phase until SB to 428.6 pmol/g DW. The maximum oxIAA content was reached at tight and open cluster, with 614 pmol/g DW on average. There is evidence, suggesting that amino acid conjugates of IAA play a vital role in auxin homeostasis. The conjugation with aspartic acid to make indole-3-acetyl aspartic acid (IAAsp) is irreversible. The content of IAAsp (Table 6) was low during endodormancy (84.3 pmol/g DW). Remarkably to this metabolite is the transient ninefold increase of conjugation during ecodormancy and early ontogenetic development between t_1* and swollen bud, which led to 777.2 and 649.8 pmol/g DW IAAsp. During the visible developmental stages between side green and tight cluster, the values decreased again, to 66 pmol/g DW IAAsp on average, comparable to the value during endodormancy (LF-t_1). The most well-known pathway involves the conjugation of IAA to amino acids by the GH3 gene family. Most amino acid conjugates can be hydrolyzed by the ILR1/ILL gene family to release free IAA. These conjugates are sometimes called "storage forms" or "bound" auxin (Kramer and Ackelsberg 2015 and references therein).

The ratio of IAAsp/oxIAA of 3.57 (Table 6) was significantly higher during eco-dormancy compared to the

Table 1 Content of active CKs – free bases (iP, *t*Z, *c*Z, DHZ) in sweet cherry buds during different phases and at different phenological stages

Phase/Stage	iP (pmol/g DW)	*t*Z (pmol/g DW)	*c*Z (pmol/g DW)	DHZ (pmol/g DW)
LF – t_1	2.2 ± 0.1^{b}	1.3 ± 0.3^{b}	2.0 ± 0.1^{b}	0.7 ± 0.1^{b}
t_1 – t_1*	4.8 ± 0.4^{ab}	1.6 ± 0.2^{b}	2.3 ± 0.1^{b}	0.7 ± 0.1^{b}
t_1* – SB	6.3 ± 1.0^{a}	4.1 ± 1.3^{a}	3.7 ± 0.3^{a}	1.2 ± 0.1^{a}
SG	13.1 ± 1.2^{A}	9.4 ± 0.1^{A}	6.4 ± 0.2^{A}	0.9 ± 0.1^{B}
GT	25.1 ± 6.4^{A}	21.1 ± 8.3^{A}	5.6 ± 1.4^{A}	2.9 ± 0.3^{B}
TC	11.4 ± 3.0^{A}	40.6 ± 16.3^{A}	8.0 ± 2.2^{A}	8.4 ± 0.4^{A}
OC	9.2 ± 1.8^{A}	23.1 ± 8.1^{A}	7.0 ± 1.4^{A}	7.1 ± 0.9^{A}

Mean ± SE 2012/13 and 2013/14, ANOVA, Scheffé's procedure; different small letters indicate significance ($p < 0.05$) between phenological phases and capitals between phenological stages

Table 2 Content of active CKs – and their respective ribosides (iPR, *t*ZR, *c*ZR, DHZR) in sweet cherry buds during different phases and at different phenological stages

Phase/Stage	iPR (pmol/g DW)	*t*ZR (pmol/g DW)	*c*ZR (pmol/g DW)	DHZR (pmol/g DW)
LF – t_1	8.2 ± 0.4^{b}	3.4 ± 0.2^{b}	9.8 ± 0.6^{b}	3.1 ± 0.3^{b}
t_1 – t_1*	9.1 ± 0.8^{b}	4.3 ± 0.5^{b}	10.8 ± 0.8^{b}	4.1 ± 0.1^{a}
t_1* – SB	25.0 ± 3.1^{a}	8.0 ± 0.9^{a}	24.1 ± 3.2^{a}	4.3 ± 0.5^{a}
SG	49.0 ± 2.6^{B}	13.3 ± 0.2^{B}	69.3 ± 3.4^{A}	8.2 ± 0.1^{C}
GT	311.8 ± 19.9^{A}	432.5 ± 214.8^{A}	165.3 ± 21.4^{A}	30.2 ± 1.5^{C}
TC	281.7 ± 45.9^{A}	462.3 ± 63.7^{A}	239.6 ± 50.8^{A}	116.6 ± 9.6^{A}
OC	169.6 ± 23.1^{AB}	200.9 ± 27.5^{AB}	230.8 ± 43.7^{A}	85.1 ± 3.0^{B}

Mean ± SE 2012/13 and 2013/14, ANOVA, Scheffé's procedure; different small letters indicate significance ($p < 0.05$) between phenological phases and capitals between phenological stages

Table 3 Content of sugar conjugates-N9-glucosides and *O*-glucosides (iP9G, *t*ZOG, *c*ZOG, DHZOG) in sweet cherry buds during different phases and at different phenological stages

Phase/Stage	iP9G (pmol/g DW)	*t*ZOG (pmol/g DW)	*c*ZOG (pmol/g DW)	DHZOG (pmol/g DW)
LF – t_1	0.6 ± 0.03^{a}	38.1 ± 1.3^{a}	28.0 ± 2.4^{c}	24.6 ± 1.3^{b}
t_1 – t_1*	0.7 ± 0.01^{a}	41.2 ± 5.2^{a}	45.7 ± 1.3^{b}	26.4 ± 0.5^{ab}
t_1* – SB	0.7 ± 0.04^{a}	43.2 ± 2.5^{a}	65.0 ± 3.0^{a}	28.6 ± 1.7^{a}
SG	0.6 ± 0.04^{A}	86.4 ± 10.5^{A}	107.4 ± 17.3^{A}	25.4 ± 0.4^{A}
GT	0.5 ± 0.05^{A}	57.9 ± 8.1^{A}	75.3 ± 5.7^{B}	28.0 ± 2.4^{A}
TC	0.5 ± 0.05^{A}	66.8 ± 9.9^{A}	46.0 ± 1.6^{C}	32.7 ± 3.2^{A}
OC	0.5 ± 0.09^{A}	71.0 ± 16.0^{A}	39.3 ± 2.8^{C}	27.8 ± 0.9^{A}

Mean ± SE 2012/13 and 2013/14, ANOVA, Scheffé's procedure; different small letters indicate significance ($p < 0.05$) between phenological phases and capitals between phenological stages

ecodormancy or the phase from t_1* until swollen bud, 0.45, and 1.64, respectively. This indicates strong involvement of genes in sweet cherry buds responsible for conjugation with aspartic acid to make indole-3-acetyl aspartic acid (IAAsp), and are involved to maintain ecodormancy at a mean temperature of 1.6 °C during this phase. Our results agree with the general picture that emerges from the work of Kramer and Ackelsberg (2015) on seed plants, that auxin accumulation in a nascent sink tissue upregulates auxin conjugation, preventing auxin toxicity and limiting the size of the region subject to auxin-mediated gene activation. Compared to the ratio of 0.34 at SG, the ratio of IAAsp/oxIAA decreased subsequently to the mean of 0.08, indicating decreasing importance of conjugation of IAA with aspartic acid during the later phenological bud development (GT-TC) (Table 6).

Table 4 Content of sugar conjugates-riboside-*O*-glucosides (*t*ZROG, *c*ZROG, DHZROG) in sweet cherry buds during different phases and at different phenological stages

Phase/Stage	*t*ZROG (pmol/g DW)	*c*ZROG (pmol/g DW)	DHZROG (pmol/g DW)
LF – t_1	1.2 ± 0.2^{ab}	1.5 ± 0.1^{b}	1.5 ± 0.2^{a}
t_1 – t_1*	1.2 ± 0.7^{ab}	2.1 ± 0.1^{b}	1.5 ± 0.1^{a}
t_1* – SB	1.7 ± 0.1^{a}	3.3 ± 0.2^{a}	1.7 ± 0.2^{a}
SG	1.8 ± 0.1^{C}	3.4 ± 0.2^{B}	4.0 ± 0.3^{AB}
GT	7.9 ± 1.1^{CB}	6.1 ± 0.3^{B}	6.7 ± 1.6^{AB}
TC	27.0 ± 2.0^{A}	10.1 ± 0.7^{A}	15.9 ± 2.2^{A}
OC	14.2 ± 0.6^{AB}	10.9 ± 1.1^{A}	11.6 ± 1.2^{AB}

Mean ± SE 2012/13 and 2013/14, ANOVA, Scheffé's procedure; different small letters indicate significance ($p < 0.05$) between phenological phases and capitals between phenological stages

Conclusion

This study, focussed on sweet cherry buds, revealed that no changes in the content of different bioactive metabolites of GAs (exception GA_3), CKs, and AX occurred during winter rest, and more precisely, during endo- and ecodormancy. These metabolites, therefore, are not suitable to differentiate between these dormancy phases. Remarkably and unexpectedly, for the member of these groups of plant hormones, the proposed hypothesis for sweet cherry flower buds is thus in the statistically sense rejected. The beginning of ontogenesis or morphogenesis, which can be defined as an intra-organismal process by which genotype becomes phenotype, or by which an undifferentiated organism becomes a highly complex, highly differentiated organism (Walsh 2007), is accompanied by specific changes of the content of bioactive molecules, precursors, and conjugation products of the examined phytohormones.

Acknowledgements The authors (DT, AP, ON) give sincere thanks to Hana Martinková and Magdalena Vlčková for their excellent technical assistance. The work was supported by the ERDF project "Plants as a tool for sustainable global development" (No. CZ.02.1.01/0.0/0.0/16_019/0000827) and "Centre for Experimental Plant Biology" (No. CZ.02.1.01/0.0/0.0/16_019/0000738).

Author Contributions KPG and FMC contributed equally to writing, reviewing and editing the paper; DT, AP, ON were responsible for plant hormone analysis and critically revision of the manuscript. All authors have read and agreed to the published version of the manuscript.

Funding Open Access funding enabled and organized by Projekt DEAL. This work was supported by the German Research Foundation (DFG) in the project "Profiling as method to identify relevant metabolites for phenological modelling purposes" by the grant CH 228/7–1.

Table 5 Content of different total CK types in sweet cherry buds during different phases and at different phenological stages

Phase/Stage	Total iP-type (pmol/g DW)	Total *t*Z-type (pmol/g DW)	Total *c*Z-type (pmol/g DW)	Total DHZ-type (pmol/g DW)	Total CK bases (pmol/g DW)	Total CK ribosides (pmol/g DW)	Total CK nucleotides (pmol/g DW)	Total CK *O*-Glucosides (pmol/g DW)	Total CK *N*-Glucosides (pmol/g DW)	Total CKs (pmol/g DW)
LF – t_1	14.5 ± 0.8^{b}	48.5 ± 1.7^{b}	56.8 ± 2.8^{c}	32.5 ± 2.0^{a}	6.2 ± 0.4^{b}	25.3 ± 1.6^{b}	21.3 ± 1.8^{b}	102.0 ± 8.5^{b}	1.3 ± 0.04^{b}	158.0 ± 10.2^{b}
t_1 – t_1*	19.7 ± 1.6^{b}	51.2 ± 6.0^{b}	79.0 ± 2.1^{b}	32.5 ± 0.6^{a}	9.4 ± 0.7^{b}	27.3 ± 1.4^{b}	28.3 ± 1.2^{b}	115.0 ± 2.5^{b}	1.4 ± 0.02^{b}	179.4 ± 4.6^{b}
t_1* – SB	43.7 ± 4.2^{a}	67.9 ± 4.3^{a}	123.5 ± 3.9^{a}	35.5 ± 1.9^{a}	15.2 ± 2.5^{a}	61.4 ± 7.3^{a}	50.1 ± 2.0^{a}	139.5 ± 4.4^{a}	1.7 ± 0.04^{a}	268.0 ± 10.9^{a}
SG	74.6 ± 3.6^{C}	124.1 ± 10.1^{B}	209.8 ± 19.6^{A}	40.4 ± 0.7^{B}	29.8 ± 1.7^{A}	140.3 ± 3.4^{C}	49.0 ± 1.0^{B}	228.5 ± 26.8^{A}	1.4 ± 0.04^{A}	448.9 ± 25.4^{C}
GT	362.5 ± 22.5^{A}	554.7 ± 133.1^{A}	274.1 ± 27.1^{A}	69.2 ± 4.1^{B}	54.7 ± 16.0^{A}	939.9 ± 127.6^{AB}	82.4 ± 10.3^{AB}	182.0 ± 13.5^{A}	1.5 ± 0.12^{A}	1260.4 ± 117.4^{AB}
TC	313.5 ± 48.0^{AB}	650.4 ± 39.7^{A}	320.7 ± 52.2^{A}	176.4 ± 15.7^{A}	68.4 ± 21.3^{A}	1100.2 ± 56.1^{A}	91.5 ± 6.7^{A}	199.4 ± 16.8^{A}	1.5 ± 0.08^{A}	1461.0 ± 82.2^{A}
OC	195.7 ± 23.3^{BC}	347.1 ± 20.7^{AB}	303.5 ± 42.0^{A}	133.6 ± 2.9^{A}	46.5 ± 10.5^{A}	686.4 ± 40.9^{B}	70.4 ± 7.1^{AB}	174.1 ± 19.0^{A}	1.5 ± 0.08^{A}	979.0 ± 62.7^{B}

Mean ± SE, 2012/13 and 2013/14, ANOVA, Scheffé's procedure; different small letters indicate significance ($p < 0.05$) between phenological phases and capitals between phenological stages

Table 6 Content of IAA, oxIAA, IAAsp, and the ratio of IAAsp/oxIAA in sweet cherry buds during different phases and at different phenological stages

Phase/Stage	IAA (pmol/g DW)	oxIAA (pmol/g DW)	IAAsp (pmol/g DW)	Ratio IAAsp/oxIAA
LF – t_1	290.7 ± 25.7^{ab}	246.9 ± 27.2^{b}	84.3 ± 9.4^{b}	0.45 ± 0.09^{b}
t_1 – t_1*	246.0 ± 14.6^{b}	232.2 ± 11.3^{b}	777.2 ± 53.6^{a}	3.57 ± 0.34^{a}
t_1* – SB	337.1 ± 32.6^{a}	428.6 ± 36.4^{a}	649.8 ± 55.6^{a}	1.64 ± 0.24^{b}
SG	174.7 ± 25.3^{A}	288.9 ± 57.1^{B}	98.9 ± 9.8^{A}	0.34 ± 0.05^{A}
GT	335.8 ± 45.0^{A}	427.7 ± 97.9^{AB}	53.6 ± 20.1^{A}	0.07 ± 0.02^{B}
TC	403.0 ± 96.7^{A}	617.6 ± 25.3^{A}	42.8 ± 6.9^{A}	0.06 ± 0.01^{B}
OC	556.2 ± 113.0^{A}	611.2 ± 49.5^{A}	70.3 ± 8.4^{A}	0.11 ± 0.01^{B}

Mean ± SE 2012/13 and 2013/14, ANOVA, Scheffé's procedure; different small letters indicate significance ($p < 0.05$) between phenological phases and capitals between phenological stages

Declarations

Conflict of interest All the authors declare that there is no competing interest in this manuscript.

References

Barboza-Barquero L, Nagel KA, Jansen M, Klasen JR, Kastenholz B, Braun S, Bleise B, Brehm T, KoornneefM FF (2015) Phenotype of *Arabidopsis thaliana* semi-dwarfs with deep roots and high growth rates under water-limiting conditions is independent of the GA5 loss-of-function alleles. Ann Bot 116:321–331

Beauvieux R, Wenden B, Dirlewanger E (2018) Bud dormancy in perennial fruit tree species: a pivotal role for oxidative cues. Front Plant Sci 16:657

Campos-Rivero G, Osorio-Montalvo P, Sánchez-Borges R, Us-Camas R, Duarte-Aké F, De-la-Peña C (2017) Plant hormone signaling in flowering: an epigenetic point of view. J Plant Physiol 214:16–27

Campoy JA, Ruiz D, Egea J (2011) Dormancy in temperate fruit trees in a global warming context: a review. Sci Hortic 130:357–372

Chmielewski FM, Götz KP (2017) Identification and timing of dormant and ontogenetic phase for sweet cherries in Northeast Germany for modelling purposes. J Hortic 4:205. https://doi.org/10.4172/2376-0354.1000205

Dobrev PI, Kamínek M (2002) Fast and efficient separation of cytokinins from auxin and abscisic acid and their purification using mixed-mode solid-phase extraction. J Chromatogr 950:21–29

Götz KP, Chmielewski FM, Homann T, Huschek G, Matzneller P, Rawel HM (2014) Seasonal changes of physiological parameters in sweet cherry (*Prunus avium* L.) buds. Sci Hortic 172:183–190

Hedden P, Phillips AL (2000) Gibberellin metabolism: new insights revealed by the genes. Trends Plant Sci 12:523–530

Hedden P, Thomas SG (2012) Gibberellin biosynthesis and its regulation. Biochemical Journal 444:11–25

Kang J, Lee Y, Sakakibara H, Martinoia E (2017) Cytokinin transporters: GO and STOP in signaling. Trends in Plant Sci 22(6):455

Koutinas N, Pepelyankov G, Lichev V (2010) Flower induction and flower bud development in apple and sweet cherry. Biotechnol Biotechnol Equip 24:1549–1558

Kramer EM, Ackelsberg EM (2015) Auxin metabolism rates and implications for plant development. Front Plant Sci 6:150

Novák O, Hauserová E, Amakorová P, Doležal K, Strnad M (2008) Cytokinin profiling in plant tissues using ultra-performance liquid chromatography-electrospray tandem mass spectrometry. Phytochemistry 69:2214–2224

Novák O, Hényková E, Sairanen I, Kowalczyk M, Pospíšil T, Ljung K (2012) Tissue-specific profiling of the *Arabidopsis thaliana* auxin metabolome. Plant J 72:523–536

Pielot R, Kohl S, Manz B, Rutten T, Weier D, Tarkowská D, Rolčík J, Strnad M, Volke F, Weber H, Weschke W (2015) Hormone-mediated growth dynamics of the barley pericarp as revealed by magnetic resonance imaging and transcript profiling. J Exp Bot 66:6927–6943

Rijavec T, Dermastia M (2010) Cytokinins and their function in developing seeds. Acta Chim Slov 57:617–629

Rittenberg D, Foster L (1940) A new procedure for quantitative analysis by isotope dilution, with application to the determination of amino acids and fatty acids. J Biol Chem 133:727–744

Schäfer M, Brütting C, Meza-Canales ID, Großkinsky DK, Vankova R, Baldwin IT et al (2015a) The role of *cis*zeatin-type cytokinins in plant growth regulation and mediating responses to environmental interactions. J Exp Botany 66(16):4873–4884

Schäfer M, Meza-Canales ID, Navarro-Quezada A, Brütting C, Vanková R, Baldwin IT, Meldau S (2015b) Cyto-kinin levels and signaling respond to wounding and the perception of herbivore elicitors in *Nicotiana attenuate*. J Integr Plant Biol 57(2):198–212

Schmülling T (2004) Cytokinin. In: Lennarz W, Lane MD (eds) Encyclopedia of Biological Chemistry. Academic Press/Elsevier Science, USA

Smith SM, Li C, Li J (2017) Hormone function in plants. In: Hormone Metabolism and Signaling in Plants. © Li J, Chuanyou Li C, Smith S. Published by Elsevier Ltd https://doi.org/10.1016/B978-0-12-811562-6.00001-3

Urbanová T, Tarkowská D, Novák O, Hedden P, Strnad M (2013) Analysis of gibberellins as free acids by ultra- performance liquid chromatography-tandem mass spectrometry. Talanta 112:85–94

Van der Schoot C, Paul LK, Päivi L, Rinne H (2014) The embryonic shoot: a lifeline through winter. J Exp Botany 65(7):1699–1712

Walsh DM (2007) Development: three grades of ontogenetic involvement. Handbook of the philosophy of science. In: Philosophy of Biology. Elservier B.V. (Eds) Gabby DM, Thagard P, Stephens

Weier D, Thiel J, Kohl S, Tarkowská D, Strnad M, Schaarschmidt S, Weschke W, Weber H, Hause B (2014) Gibberellin-to-abscisic

acid balances govern development and differentiation of the nucellar projection of barley grains. J Exp Bot 65:(18)5291–5304
Yamaguchi S (2008) Gibberellin metabolism and its regulation. Annu Rev Plant Biol 59:225–251
Yu S, Galvão VC, Zhang YC, Horrer D, Zhang TQ, Hao YH, Feng YQ, Wang S, Schmid M, Wanga JW (2012) Gibberellin regulates the Arabidopsis floral transition through miR156-targeted SQUAMOSA PRO MOTER BINDING-LIKE transcription Factors. Plant Cell 24:3320–3332
Zalabák D, Pospíšilová H, Šmehilová M, Mrízová K, Frébort I, Galuszka P (2013) Genetic engineering of cyto-kinin metabolism: Prospective way to improve agricultural traits of crop plants. Biotechnol Adv 31:97–117
Zhang J, Peer WA (2017) Auxin homeostasis: the DAO of catabolism. J Exp Botany 68(12):3145–3154
Zhao Y (2010) Auxin biosynthesis and its role in plant development. Annu Rev Plant Biol 61:49–64